CHEMISTRY
A EUROPEAN JOURNAL

Assembly of Heteropoly Acid Nanoparticles in SBA-15 and Its Performance as an Acid Catalyst

Shu-Yuan Yu, Li-Ping Wang, Bo Chen, Ying-Ying Gu, Jing Li, Han-Ming Ding, and Yong-Kui Shan*[a]

Abstract: Keggin-type 12-tungstophosphoric acid (TPA) nanocrystals have been assembled inside the pores of mesoporous silica through a vacuum impregnation method by using large-pore SBA-15 as a nanoreactor. The product was characterized by Brunauer–Emmet–Teller particle size distribution (BET-PSD), NMR and FT-IR spectroscopy, X-ray diffraction (XRD), tranmsission electron microscopy (TEM), differential thermal analysis (DTA) and FT-IR of adsorbed pyridine. The experimental results illustrate that the TPA nanocrystals are excellent Brønsted acid catalytic materials at room temperature.

Keywords: dimerization · heteropoly acids · mesoporous silica · nanostructures · vacuum

Introduction

Many efforts have been dedicated to the utilization of mesoporous materials as nanoreactors to prepare monodispersive nanoparcticles or nanowires of uniform size, because of the "particle-sieving effect" of mesoporous materials.[1–4] Many nanoparticles or nanowires have been encapsulated into the channels of mesoporous materials, such as Ge,[5] Ag,[6] Pd,[7] Fe_2O_3,[8] GaAs,[9] Ru–Ag,[10] and ruthenium–carbonyl complexes,[11] by incorporation of inorganic precursors into the channels by sorption, phase transition, ion exchange, complex or covalent grafting, impregnation, and gas-phase chemical-vapor infiltration or deposition with further treatment. The mesopores or channels can be regarded as hosts and the nanoparticles or nanowires as guests like in the host–guest chemistry. In addition, all of these nanoparticles or nanowires are composed of mono- or bimetal elements or binary compounds or complexes; nanoparticles containing more than two components have not been found in literature. The reason may be that incorporation of multiple component compounds into the pore canals of porous materials is more difficult than that of mono- or binary compounds. Pure heteropoly acids, generally containing at least four different types of elements, are obtained by the condensation of two or more different types of related oxoanions in an acidic solution followed by extraction under acidic conditions. Heteropoly acids exist as an equilibrium system of many species in the synthetic procedures, which makes the aforementioned methods unsuitable for the preparation of the pure heteropoly acid nanocrystals inside channels of porous materials. Although the conventional wet impregnation method may incorporate some heteropoly acid molecules into the channels of mesoporous materials, the amount of heteropoly acid is too small to form nanocrystals.[11–13]

There are three important prerequisites for the confinement of the heteropoly acid nanoparticles inside the pores of porous materials. Firstly, the size of the pores must be large enough to accommodate the heteropoly acid nanoparticles. Secondly, the amount of heteropoly acid incorporated into the pores should be enough. Thirdly, conditions of crystallization have to be mild to prevent the loss of water of crystallization. Therefore, our synthetic strategy was to use the mesoporous silica SBA-15 with large pore diameter as a host for limiting the growth of crystals inside the pores; to apply high-vacuum (10^{-7} Torr) pretreatment for clearing water molecules, nitrogen, and other contaminations from the pores of the SBA-15 in order to provide more capacity; and to finish crystallization of heteropoly acid at relatively low temperature. In this way, we have successfully synthesized heteropoly acid nanoparticles within the channels of mesoporous silica SBA-15.

[a] S.-Y. Yu, L.-P. Wang, B. Chen, Y.-Y. Gu, J. Li, H.-M. Ding, Prof. Y.-K. Shan
Department of Chemistry, East China Normal University
North Zhongshan Road 3663, Shanghai 200062 (China)
Fax: (+86) 216-223-3503
E-mail: ykshan@chem.ecnu.edu.cn

DOI: 10.1002/chem.200401047

Results and Discussion

12-Tungstophosphotic acid (TPA, $H_3[PW_{12}O_{40}]$) was selected as the heteropoly acid. The diameter of the Keggin-type molecule is about 1 nm. Six loadings of TPA on SBA-15 ranging from 23–78 wt % were prepared.

The nitrogen adsorption–desorption isotherms and pore size distribution at 77 K as shown in Figure 1 are of type IV

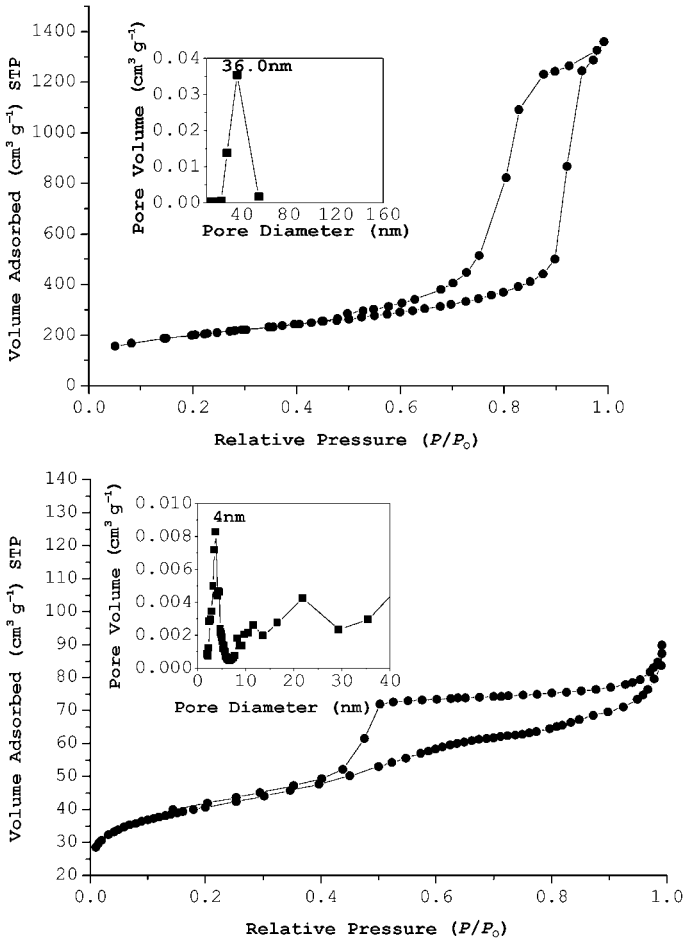

Figure 1. Nitrogen adsorption–desorption isotherm plots and pore size distribution curve for SBA-15 (top) and TPA_{60}/SBA-15v (bottom).

classification for SBA-15 and TPA_{60}/SBA-15v, which shows that both SBA-15 and TPA_{60}/SBA-15v possess the character of a mesoporous framework. The SBA-15 matrix has regular mesoporous channels and a narrow gaussian pore size distribution; its Brunauer–Emmet–Teller (BET) surface area and pore volume are 760 $m^2 g^{-1}$ and 2.1 $cm^3 g^{-1}$, respectively, and the pore diameters calculated by the Barrett–Joyner–Halenda (BJH) method are in the range of 23–55 nm. The average pore size is approximately 36 nm. Figure 1b demonstrates that the pore structure was preserved during the TPA assembly process in the channels of SBA-15, but the BET surface area, pore volume, and pore diameters decreased sharply to 143 $m^2 g^{-1}$, 0.14 $cm^3 g^{-1}$, and 2–7 nm, respectively. A well-defined step associated with the filling of the mesopores due to capillary condensation occurs approximately at $P/P_0 = 0.45$–1.00 in TPA_{60}/SBA-15v and at $P/P_0 = 0.70$–1.00 in SBA-15. These phenomena can be attributed to the encapsulation of TPA inside the channels of SBA-15, and furthermore, the high loading of about 60 wt % (determined by inductively coupled plasma (ICP) measurements) may lead to a partial blocking of the pores.

A ^{31}P chemical shift of $\delta = -15.4$ ppm is observed by NMR spectroscopy (Figure 2), which is just the same as that of the bulk TPA.[14] It indicates that the crystals of TPA exist in the pores of SBA-15 matrix and the structure of the TPA did not experience modifications during the assembly

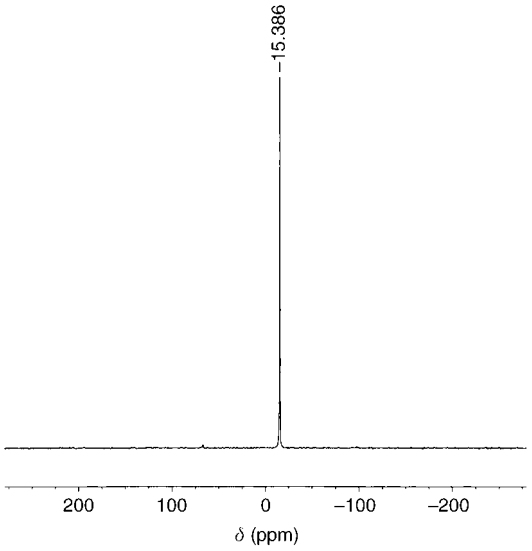

Figure 2. ^{31}P NMR MAS spectrum of TPA_{60}/SBA-15v.

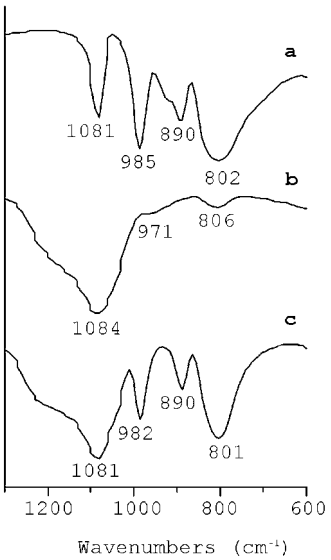

Figure 3. FT-IR spectrum of a) bulk TPA, b) SBA-15, and c) TPA_{60}/SBA-15v.

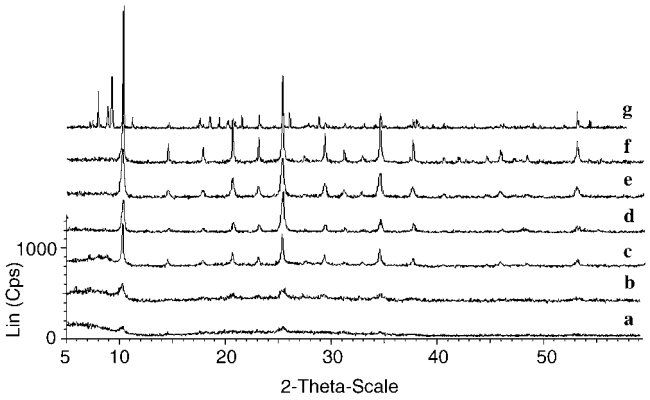

Figure 4. XRD patterns for a) TPA_{23}/SBA-15v, b) TPA_{46}/SBA-15v, c) TPA_{60}/SBA-15v, d) TPA_{67}/SBA-15v, e) TPA_{73}/SBA-15v, f) TPA_{78}/SBA-15v, and g) bulk TPA.

process; this result is different from those obtained by means of common silica impregnation.[13,15,16]

The FT-IR spectra for TPA_{60}/SBA-15v and bulk TPA are shown in Figure 3. For the bulk TPA, characteristic bands are observed at 1081 (P–O), 985 (W=O), 890 (W-O-W_{corner}), and 802 cm^{-1} (W-O-W_{edge}), which coincide with those reported in the literature for the $[PW_{12}O_{40}]^{3-}$ Keggin unit.[17] The bands of TPA_{60}/SBA-15v appear at 1081, 982, 890, and 801 cm^{-1} without overlapping, which are also a good proof of the existence of the Keggin structure $[PW_{12}O_{40}]^{3-}$ anions without depolymerization or degradation.

The XRD patterns for bulk TPA and TPA/SBA-15v are displayed in Figure 4. No signal is detected in the small-angle range for the large-pore SBA-15 matrix. The crystal diffraction signals for the crystalline phase of TPA are perfectly offered by TPA/SBA-15v samples with a TPA loading of 60 wt% and higher in the 2θ region from 5 to 60° and the broadening of these signals can be clearly seen in the patterns. This broadening reveals that the TPA crystals are on the nanoscale size, and the average crystal size calculated by the Scherrer formula is about 20 nm, which is consistent with the pore diameter of the SBA-15 matrix. The XRD patterns show that by using the large-pore SBA-15 as a nanoreactor, the Keggin structure TPA nanoparticles can be prepared easily in the channels when the loading is approximately 60 wt% by the new vacuum impregnation method. In earlier research, it was shown that no TPA crystal phase exits in the TPA/SBA-15 materials prepared by traditional wet impregnation below TPA loadings of 80%.[18–20]

The TEM images for SBA-15 and TPA/SBA-15v and TPA/SBA-15i samples are presented in Figure 5a-f. SBA-15 (Figure 5a) has channels with very large diameters, into which TPA molecules can enter easily. TPA nanoparticles can be found both in the pores and on the surface of the matrix in TPA_{60}/SBA-15v samples (Figure 5b,c); however, most of the nanoparticles are distributed in the channels. As the loading is increased, more TPA nanoparticles are formed on the surface of the matrix, as shown in Figure 5d. The crystal sizes of the TPA nanoparticles, both inside and outside the pores, estimated from TEM image (Figure 5b–d) are in agreement with those calculated from XRD. In addition no TPA nanoparticles are observed in the pores or on the surface of the matrix in the TPA_{74}/SBA-15i sample (Figure 5e). The results suggest that TPA nanoparticles can just

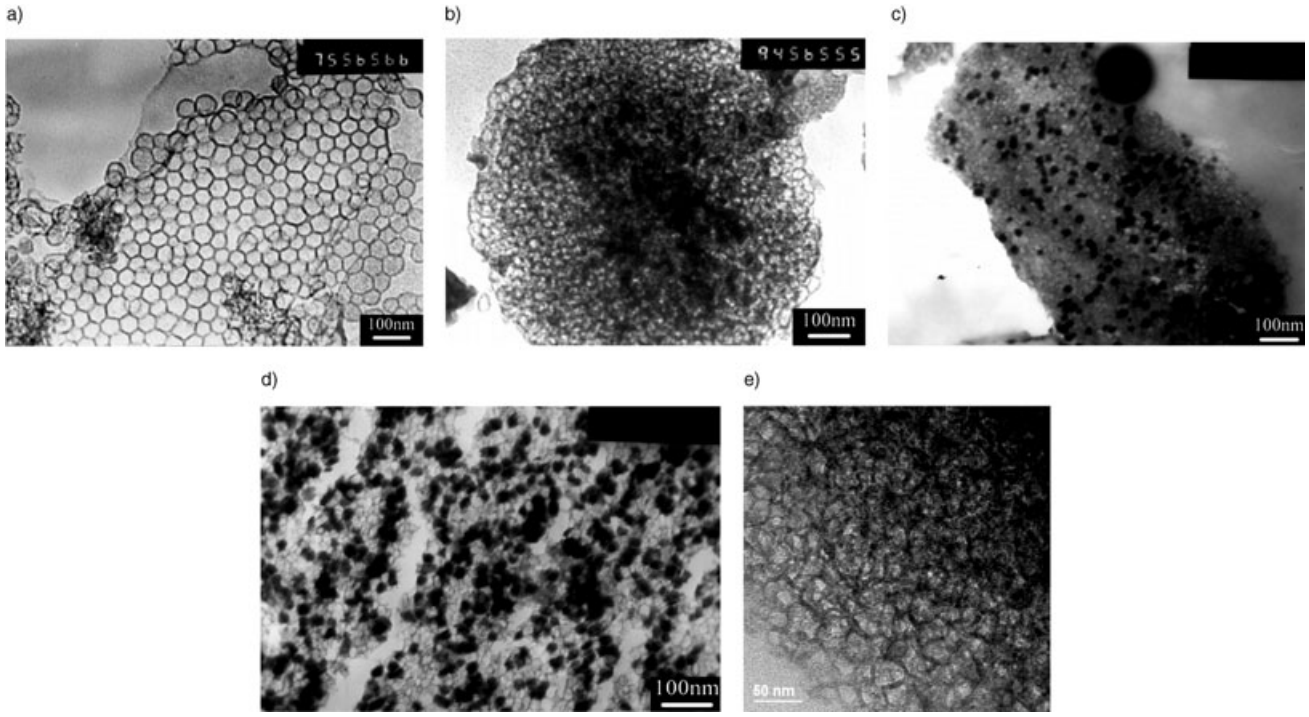

Figure 5. TEM images for large-pore SBA-15 (a), TPA_{60}/SBA-15v (b,c), TPA_{73}/SBA-15v (d), and TPA_{74}/SBA-15i (e).

be assembled in the channels of the large-pore SBA-15 through the vacuum impregnation method.

Thermal stability of TPA/SBA-15v has also been investigated by XRD. The results show that the TPA nanoparticles are quite stable up to 410 °C and degrade completely at 460 °C due to the destruction of the TPA Keggin structure with formation of phosphate and tungsten trioxide species, similar to an earlier report.[21] The initial decomposition temperature of nanoparticles is a bit lower than that of bulk TPA (465 °C);[22] this could be attributed to the interaction between TPA and silica, which can weaken the stability of TPA.[13]

The acidity of TPA_{73}/SBA-15v and TPA_{74}/SBA-15i with the same loading of TPA was determined by FT-IR spectroscopy of adsorbed pyridine. The characteristic bands at 1540 and 1635 cm^{-1} are assigned to pyridine protonated by Brønsted acid sites, while the bands from pyridine coordinated to Lewis acid sites appear at 1450 and 1608 cm^{-1}.[23,24] The intensities of the 1450 and 1540 cm^{-1} bands are listed in Table 1. The Brønsted acid sites are estimated to be much more numerous than the Lewis acid sites in both samples, and the acidity of TPA_{73}/SBA-15v is higher than that of TPA_{74}/SBA-15i according to the intensity ratio of the bands.

Table 1. The intensity of B (1540 cm^{-1}) and L (1450 cm^{-1}) bands for TPA_{73}/SBA-15v and TPA_{74}/SBA-15i.

	T [°C]	B (1540 cm^{-1})	L (1450 cm^{-1})
TPA_{73}/SBA-15v	RT	1.928	0.912
	100	2.595	0.602
	150	2.904	0.582
	200	3.109	0.564
	250	3.106	0.548
	300	2.550	0.539
TPA_{74}/SBA-15i	RT	1.235	0.514
	100	2.098	0.285
	150	2.626	0.192
	200	3.025	0.142
	250	3.253	0.111
	300	2.985	0.119

The catalytic activities of TPA_x/SBA-15v and TPA_{74}/SBA-15i for the cyclodimerization reaction of α-methylstyrene (AMS) have been investigated. The results are shown in Table 2. The TPA_x/SBA-15v catalysts exhibit high activities. The conversions are more than 99% and the selectivity of the cyclic dimer (indan) increases with increasing the TPA loading. The maximum selectivity of indan is observed over TPA_{73}/SBA-15v. The conversion of AMS catalyzed by TPA_{73}/SBA-15v and the selectivity of indan and linear dimers are 100, 97.2, and 2.8% respectively, while those catalyzed by TPA_{74}/SBA-15i are 83.9, 46.1, and 20.3%, respectively. The TPA_x/SBA-15v catalyst has a higher activity probably due to its higher acidity. The higher selectivity might be due to its higher crystallinity.

Table 2. Cyclodimerization of α-methylstyrene catalyzed by TPA_x/SBA-15v and TPA_{74}/SBA-15i.

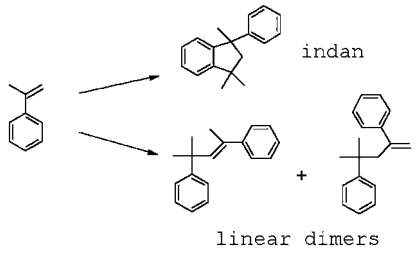

	Conversion [%]	Selectivity [%] indan	linear dimers	byproducts
TPA_{23}/SBA-15v	99.8	20.3	68.1	11.6
TPA_{46}/SBA-15v	99.0	37.0	51.5	11.5
TPA_{60}/SBA-15v	99.0	53.4	35.0	11.6
TPA_{67}/SBA-15v	99.8	89.7	3.1	7.2
TPA_{73}/SBA-15v	100	97.2	2.8	0
TPA_{78}/SBA-15v	100	66.7	27.0	6.3
TPA_{74}/SBA-15i	83.9	46.1	20.3	33.6

Conclusion

12-Tungstophosphoric acid nanoparticles with diameters of around 20 nm were successfully assembled inside the pores of large-pore SBA-15 by the novel vacuum impregnation method. We believe that this facile method of preparing tungstophosphoric acid nanoparticles could be applicable in synthesizing other multicomponent nanocrystals inside the pore system of SBA-15 and other mesoporous materials as the host for nanomanufacturing. Moreover, the tungstophosphoric acid nanoparticle system is an excellent acid catalytic material operating at low temperatures.

Experimental Section

The siliceous large-pore SBA-15 was synthesized according to the procedure reported previously.[25,26] In a typical synthesis, Pluronic P123 ($EO_{20}PO_{70}EO_{20}$) template (4.0 g) was dissolved with stirring in a solution of water (30 g) and HCl (120 g, 2 M) at 40 °C, and 1,3,5-trimethylbenzene (TMB; 6.0 g) was then added to this homogeneous solution. After 2 h, tetraethoxysilane (TEOS; 8.5 g) was also added. The resulting mixture was stirred at 40 °C for 20 h, and then aged at 100 °C for 24 h under static conditions. The as-prepared sample was recovered by filtration and air-dried. After the template was removed by calcination in air at 550 °C for 6 h, the large-pore SBA-15 (0.5 g) was pumped to a vacuum of 10^{-7} Torr with a turbo pump. An excess aqueous solution of tungstophosphoric acid (TPA) (10, 20, 30, 40, 50, 60 wt%) was introduced and kept in contact for 24 h under vacuum. Then the solution was pumped out and the solid was dried at 100 °C in air. The materials are denoted as TPA_x/SBA-15v, in which x denotes the loading amount of TPA as wt%, which was determined by ICP. TPA was also impregnated into the SBA-15 with the similar procedure except for the vacuum treatment. This sample is denoted as TPA_{74}/SBA-15i.

The cyclodimerization reaction of α-methylstyrene (AMS) was performed in a continuous flow stainless steel fixed bed microreactor system with N_2 (20 mL min^{-1}) as carrier gas. The catalyst (0.3 g) was pretreated at 100 °C for 10 h. The reaction was carried out at room temperature without extra heating.

Acknowledgements

This research was financially supported by the National Natural Science Foundation of China (No. 20173017 and 20273021).

[1] W.-H. Zhang, J.-L. Shi, H.-R. Chen, Z.-L. Hua, D.-S. Yan, *Chem. Mater.* **2001**, *13*, 648–654.
[2] H. Parala, H. Winkler, M. Kolbe, A. Wohlfart, R. A. Fischer, R. Schmechel, R. V. Seggern, *Adv. Mater.* **2000**, *12*, 1050–1055.
[3] S. J. Haswell, R. J. Middleton, B. O'Sullivan, V. Skelton, P. Watts, P. Styring, *Chem. Commun.* **2001**, 391–398.
[4] H. Yang, Q. Shi, B. Tian, Q. Lu, F. Gao, S. Xie, J. Fan, C. Yu, B. Tu, D. Zhao, *J. Am. Chem. Soc.* **2003**, *125*, 4724–4725.
[5] R. Leon, D. Margolese, G. Stucky, P. M. Petroff, *Phys. Rev. B* **1995**, *52*, 2285–2288.
[6] K.-B. Lee, S.-M. Lee, Cheon, *J. Adv. Mater.* **2001**, *13*, 517–520.
[7] M. H. Huang, A. Choudrey, P. Yang, *Chem. Commun.* **2000**, 1063–1064.
[8] T. Abe, Y. Tachibana, T. Uematsu, M. Iwamoto, *J. Chem. Soc. Chem. Commun.* **1995**, 1617–1618.
[9] V. I. Srdanov, I. Alxneit, G. D. Stucky, C. M. Reaves, S. P. DenBaars, *J. Phys. Chem. B* **1998**, *102*, 3341–3344.
[10] D. S. Shephard, T. Maschmeyer, B. F. G. Johnson, J. M. Thomas, G. Sankar, D. Ozkaya, W. Zhou, R. D. Oldroyd, R. G. Bell, *Angew. Chem.* **1997**, *109*, 2337–2341; *Angew. Chem. Int. Ed. Engl.* **1997**, *36*, 2242–2245.
[11] W. Zhou, J. M. Thomas, D. S. Shephard, B. F. G. Johnson, D. Ozkaya, T. Maschmeyer, R. G. Bell, Q. Ge, *Science* **1998**, *280*, 705–708.
[12] P. G. Vázquez, M. N. Blanco, C. V. Cáceres, *Catal. Lett.* **1999**, *60*, 205–215.
[13] L. R. Pizzio, C. V. Cáceres, M. N. Blanco, *Appl. Catal. A* **1998**, *167*, 283–294.
[14] W. L. Chu, X. G. Yang, Y. K. Shan, X. K. Ye, Y. Wu, *Catal. Lett.* **1996**, 42, 201–206.
[15] L. H. Little, *Infrared Spectra of Adsorbed Species*, Academic Press, New York, **1966**.
[16] K. Tanabe, Catalysis, *Science and Technology*, *Vol. 2* (Eds.: J. R. Anderson, M. Bondart), Springer, New York, **1981**.
[17] I. V. Kozhevnikov, K. R. Kloetstra, A. Sinnema, H. W. Zandbergen, H. V. Bekkum, *J. Mol. Catal. A* **1996**, *114*, 287–298.
[18] X. Z. Zhang, Y. H. Le, Z. Gao, *Gaodeng Xuexiao Huaxue Xuebao* **2001**, *22*, 1169–1172.
[19] Q. Y. Liu, W. L. Wu, J. Wang, X. Q. Ren, Y. R. Wang, *Microporous Mesoporous Mater.* **2004**, *76*, 51–60.
[20] J. Wang, H. O. Zhu, *Catal. Lett.* **2004**, *93*, 209–212.
[21] B. W. Southward, J. S. Vaughan, C. T. O'Connor, *J. Catal.* **1995**, *153*, 293–303.
[22] V. F. Chuvaev, K. I. Popov, V. I. Spitsyn, *Dokl. Akad. Nauk Az. SSR* **1980**, *255*, 892–898.
[23] Y. Sun, Y. Yue, H. Li, Z. Gao, *Acta Chimi*ca. *Sini*ca **1999**, 57, 746–753.
[24] C. Rocchiccioli-Deltcheff, R. Thouvenot, R. Franck, *Spectrochim. Acta Part A* **1976**, *32*, 587–591.
[25] D. Zhao, J. Feng, Q. Huo, N. Melosh, G. H. Fredrickson, B. F. Chmelka, G. D. Stucky, *Science* **1998**, *279*, 548–552.
[26] D. Y. Zhao, Q. S. Huo, J. L. Feng, B. F Chmelka, G. D. Stucky, *J. Am. Chem. Soc.* **1998**, *120*, 6024–6036.

Received: October 14, 2004
Published online: April 13, 2005